Experimental and Semiempirical Calculation Studies of Transannular Diels—Alder and Other Competing Pericyclic Reactions

Yves L. Dory,*,† Pierre Soucy,† Marc Drouin,‡ and Pierre Deslongchamps†

Contribution from the Département de chimie, Faculté des sciences, Université de Sherbrooke, Sherbrooke, Québec, Canada J1K 2R1

Received July 14, 1994®

Abstract: Several related macrocyclic trienes have been found to interconvert thermally via [1,5]sigmatropic hydrogen shifts at the diene sites. These macrocyclic trienes further undergo thermal transannular Diels—Alder cycloaddition, thus yielding complex mixtures of adducts. This difficult problem has been tackled and qualitatively solved by means of the semiempirical methods AM1 and PM3. Most of the starting material ground states have been characterized as well as all the [1,5]sigmatropic hydrogen shift and Diels—Alder transition structures. The results of these calculations indicate that some [1,5]sigmatropic hydrogen shift enthalpies of activation are within the same range of most Diels—Alder enthalpies of activation. As a result the Curtin—Hammett principle does not apply for the entire system but only on limited regions. The method proved successful in uncovering the previously missassigned identity of one of the Diels—alder adducts: an unexpected 5—6—7-membered tricycle.

Introduction

Forcasting selectivity of chemical reactions by means of Dreiding models has been widely used with great success in general and particularly in the case of transannular Diels—Alder reactions.[1] Nevertheless, many results remain almost impossible to explain by using this simple method, since the geometries investigated correspond either to the starting materials or to the products, whereas the truely significant geometries in kinetically driven reactions are the transition state structures. We report here the use of semiempirical quantum mechanics as a reliable tool to predict selectivity in the transannular Diels—Alder reaction as well as competing reaction paths whenever applicable.

TTC (*trans-trans-cis*) macrocyclic trienes have been studied in our laboratories as potential precursors of interesting tricyclic systems related to diterpenes. Thus, the triene 1a (Scheme 1) led at 80 °C to the TST (*trans-syn-trans*) tricycle 4a only, with no trace of the other possible Diels—Alder CSC adduct 5a.[2] On the other hand, the triene 1b differing only from the triene 1b by a methyl substituent on the diene moiety did not produce the corresponding Diels—Alder adducts 4b and 5b at 200 °C but rather the CTC isomeric triene 2b.[3] When the reaction with 1b was performed at 310 °C, the expected tricycles 4b and 5b were formed with two other tricycles 6b and 7b assigned as the CST and the TSC geometries.

In order to check the validity of these assignments, the macrocyclic trienes 2a, 2b, 3a, and 3b were submitted to the Diels—Alder reaction conditions (~300 °C).[3] The macrocycles 2a and 3a (R = H) led neatly to the expected adducts 6a and

7a respectively; so did the TCC macrocycle 3b (R = Me), whereas the CTC macrocycle 2b (R = Me) produced a mixture of tricycles qualitatively identical to the TTC triene case, only the ratios were different. All the tricyclic adducts were unambiguously assigned as the structures shown, apart from 5b and 6b whose identities remained hypothetical, but could be logically attributed to the CSC and CST geometries, respectively.

The aim of this work is 2-fold: first we have to rationalize the interconversion of the macrocycles. Secondly, a quantitative analysis of the product ratios is necessary.

As already suggested,[3] the macrocycles interconversion is the result of successive [1,5]sigmatropic hydrogen shifts, which are in principle reversible processes. The resulting macrocyclic trienes can then undergo irreversible Diels—Alder cycloaddition at various stages along the macrocycles interconversion scheme.

The [1,5]Sigmatropic Hydrogen Shifts

A first draft analysis of the reactions responsible for the macrocycles interconversions (Scheme 2) shows that the TTC macrocycle 1b possesses only one proton ready for sigmatropic shift. The macrocycle 8 issued from that transformation displays two such protons: the first proton shift reverts to the starting TTC macrocycle 1b whereas the second proton shift leads forward to the CTC macrocycle 2b. The CTC macrocycle 2b which now features three available protons for such shifts can then either go backward to 8 or produce two new macrocycles 9 and 10. Each of these two macrocycles has one proton ready for [1,5]sigmatropic hydrogen shift, but the presence of the neighboring chiral center gives two possible products: the former CTC macrocycle 2b or the new CCC macrocycle 11. The CCC macrocycle 11 with four available protons either gives the two known macrocycles 9 and 10 or the two macrocycles 12 and 13. As in the case of 9 and 10, the two macrocycles 12 and 13 which possess two reactive hydrogen atoms each can produce the corresponding previous CCC macrocycle 11 or the new TCC macrocycle 3b. No other [1,5]hydrogen shift can occur from the TTC macrocycle 3b.

It has been accepted that vibrationally assissted tunnelling (VAT) is playing a major part in [1,5]sigmatropic hydrogen

* To whom correspondence should be addressed. Tel: (819) 821-8219. Fax: (819) 821-7910.
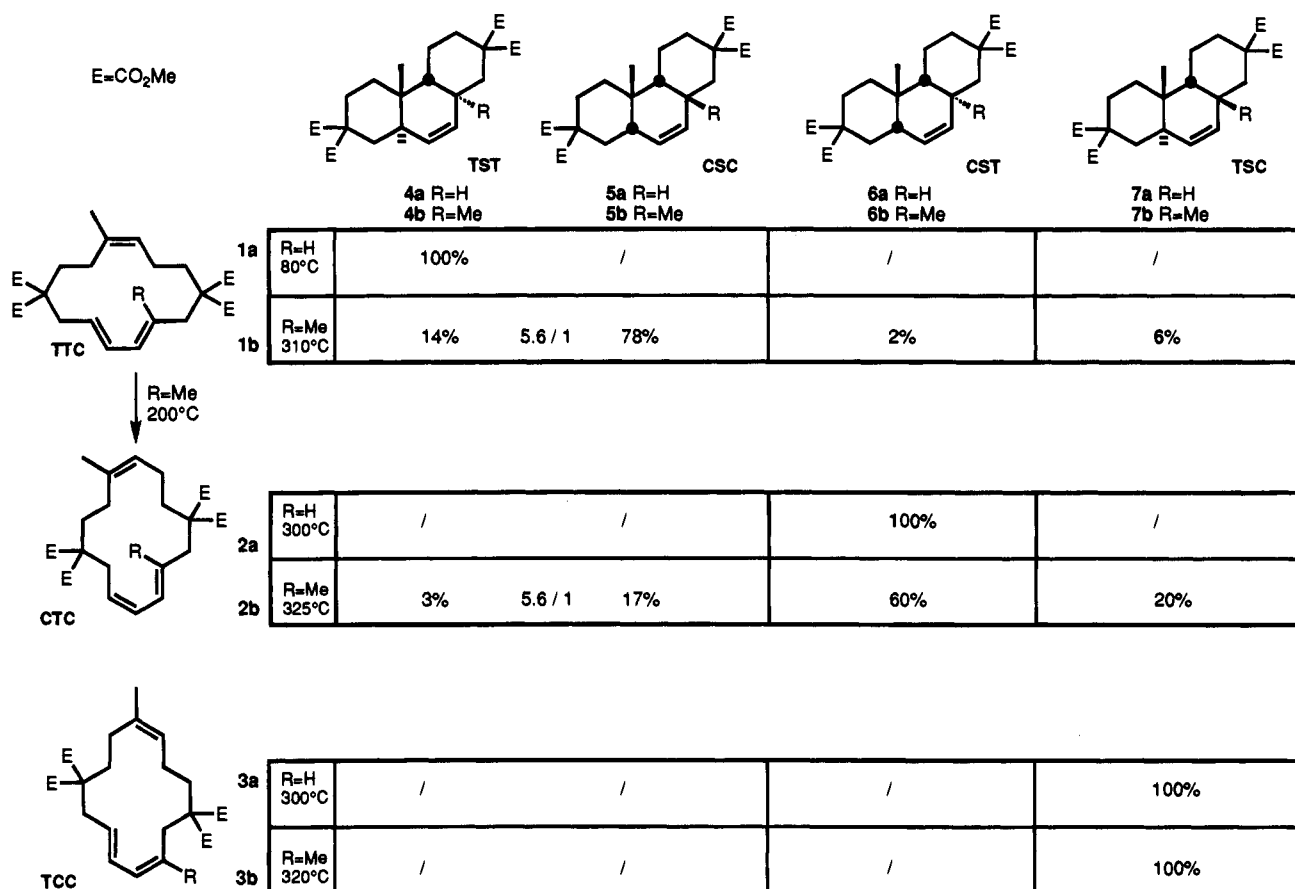† Laboratoire de synthèse organique.
‡ Laboratoire de chimie structurale.

(1) (a) Lamothe, S.; Ndibwami, A.; Deslongchamps, P. *Tetrahedron Lett.* **1988**, *29*, 1639. (b) Lamothe, S.; Ndibwami, A.; Deslongchamps, P. *Tetrahedron Lett.* **1988**, *29*, 1641.
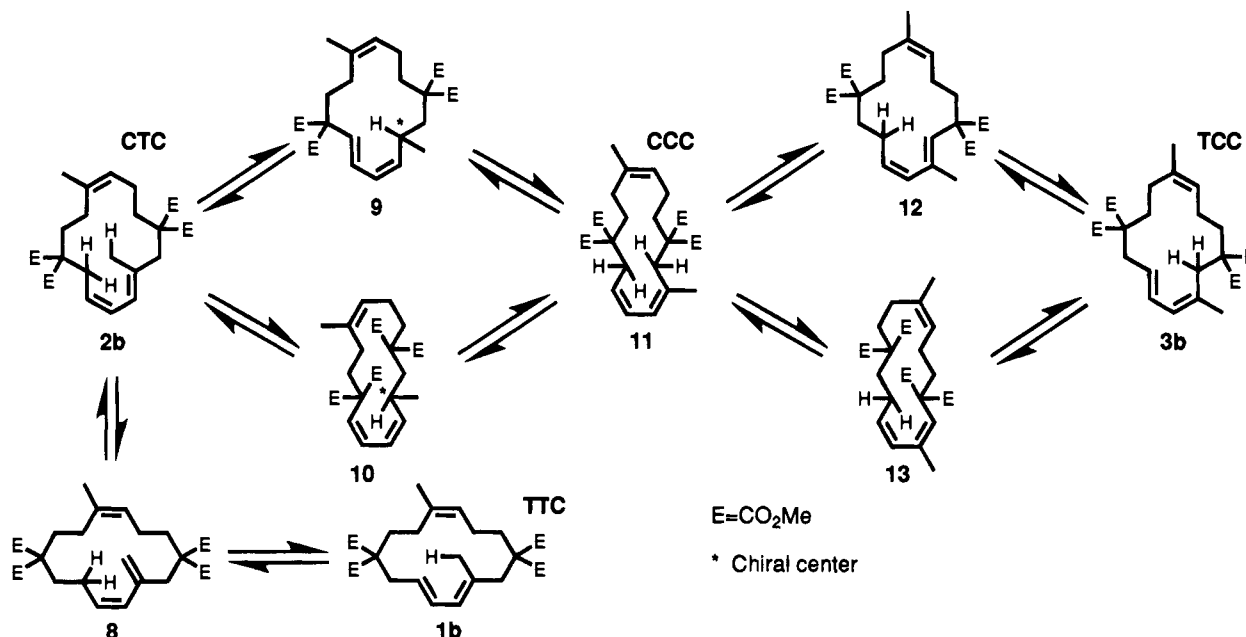(2) Ndibwami, A.; Lamothe, S.; Soucy, P.; Goldstein, S.; Deslongchamps, P. *Can. J. Chem.* **1993**, *71*, 714.
(3) Xu, Y.-C.; Roughton, A. L.; Soucy, P.; Goldstein, S.; Deslongchamps, P. *Can. J. Chem.* **1993**, *71*, 1169.

Pericyclic Reactions

J. Am. Chem. Soc., Vol. 117, No. 1, 1995 519

Scheme 1


Scheme 2

E=CO2Me

* Chiral center

shifts.[4] As a result the calculated activation energies (related to the transition states) are significantly larger than the experimental ones. Nevertheless, the transition structures are

reasonable approximations of the geometries involved in the protons VAT,[4a] since it has been demonstrated that tunneling occurs in a very small vicinity of the saddle point (transferred proton within 0.2 Å of the saddle point geometry).[4d] Moreover, since we wish to compare similar types of [1,5]sigmatropic hydrogen shifts, the transition structures should all display approximately the same energy gap as compare to their corresponding VAT backbone geometries.

(4) (a) Dewar, M. J. S.; Merz, K. M.; Stewart, J. J. P. *J. Chem. Soc., Chem. Commun.* **1985**, 166. (b) Dewar, M. J. S.; Healy, E. F.; Ruiz, J. M. *J. Am. Chem. Soc.* **1988**, *110*, 2666. (c) Chantranupong, L.; Wildman, T. A. *J. Am. Chem. Soc.* **1990**, *112*, 4151. (d) Liu, Y.-P.; Lynch, G. C.; Truong, T. N.; Lu, D.-H.; Truhlar, D. S.; Garrett, B. C. *J. Am. Chem. Soc.* **1993**, *115*, 2408.
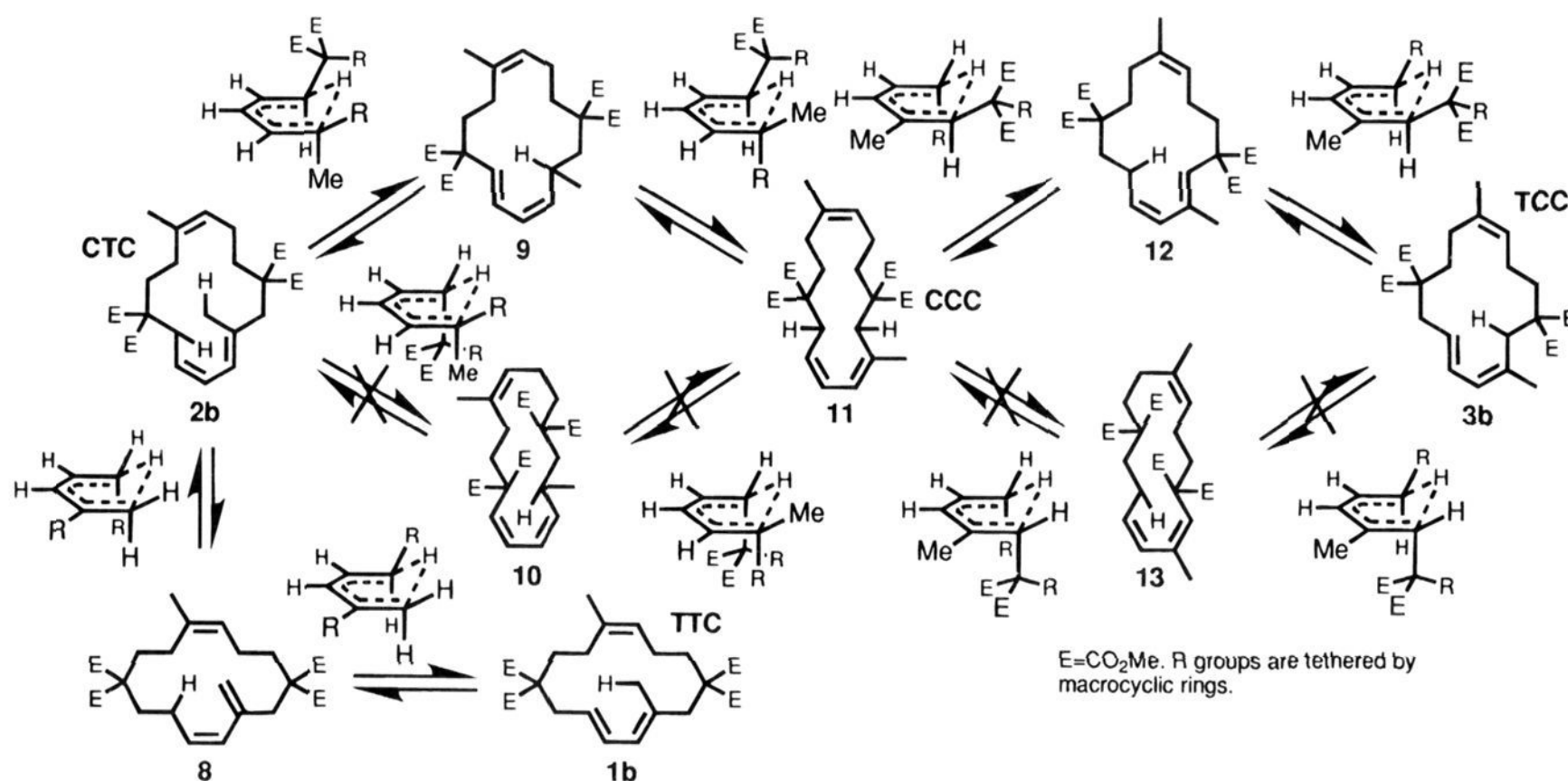
Scheme 3

TS (AM1). C---H = 1.42 Å
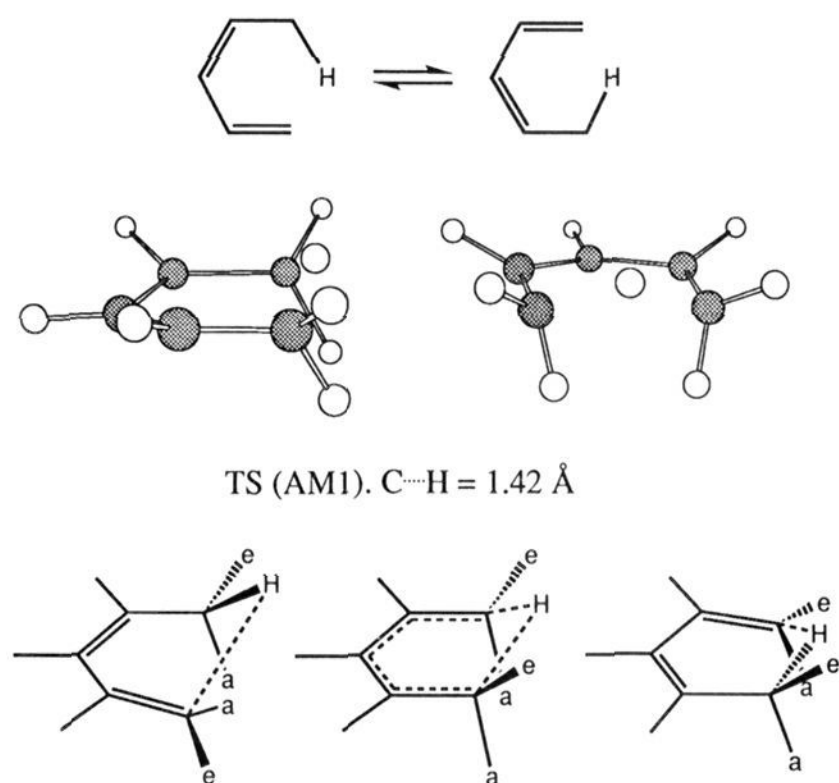
The calculations reported in the present work have been performed by means of the semiempirical Hamiltonian AM1[5] (and PM3[6] in a few cases) in MOPAC 6.0.[7,8] AM1 calculations reproduce well the experimental [1.5]hydrogen shift of (Z)-1,3-pentadiene and Diels−Alder cycloaddition of butadiene with ethene.[4d,9]

The [1,5]sigmatropic hydrogen shift transition structure of 1,3-pentadiene has been well-described in the literature.[9] Simple observation of its geometry (Scheme 3) shows that two hydrogen atoms attached to the terminal carbon atoms are axially oriented. Severe interaction may result when these protons are replaced by alkyl groups. Qualitative analysis of the 10 transition states (Scheme 4) involved in the macrocycles interconversions reveals that the transformation of the CTC macrocycle **2b** into **10** takes place via a transition state with two axial alkyl groups. Such highly disfavored geometries are also found for the transition states corresponding to the macrocycles couples **10**−**11** and **11**−**13**. As a result, those three transition states are discarded. The transition state linking both the macrocycles **13** and **3b** displays

an axial quaternary carbon center and is consequently highly disfavored, too; it will not be considered for further investigation.

The six remaining transition states A−F (Scheme 5) have all been fully characterized as well as the four ground states corresponding to the macrocycles TTC, CTC, CCC, and TCC.[10] The complexity of the problem due to the presence of four freely rotating methyl esters in the real molecules has been simplified in two ways: the four esters have been replaced by hydrogen atoms (H model) in one case and by methyl groups (Me model) in the other case, because methyl groups have no orientation problems and they can give a rough estimate of the esters steric bulk.

The AM1 calculation results (Scheme 5, Charts 1 and 2, Figures 1 and 2) account well for the CTC macrocycle greater stability over the TTC macrocycle, the energy gaps are 2.55 and 2.89 kcal/mol with the H model and the Me model, respectively. However, the H model (Chart 1) does not account for the reality since it predicts a mixture of the three macrocycles CTC **16**, CCC **18**, and TCC **20** starting from the TTC macrocycle **14**, where the TCC macrocycle would be predominant. Indeed, the transition structure B(H) responsible for the transformation of the TTC macrocycle **14** into the CTC macrocycle **16** is the highest barrier of the whole system by nearly 5 kcal/mol. Consequently, the CTC, CCC, and TCC macrocycles **16**, **18**, and **20** should equilibrate readily due to the energetically much lower transition structures C(H), D(H), E(H), and F(H). This phenomenon is not observed experimentally.

On the other hand, the Me model (Chart 2) gives rise to two barriers energetically similar in magnitude {B(Me) and D(Me); $\Delta\Delta H^{\ddagger} = 0.95$ kcal]. As a result, the activation enthalpy required to transform the TTC macrocycle **21** into its CTC isomer **23** is 48.30 kcal/mol [$\Delta H_f(B(Me)) - \Delta H_f(21)$] whereas the CTC macrocycle **23** needs 50.24 kcal/mol [$\Delta H_f(D(Me)) - \Delta H_f(23)$] to give the CCC macrocycle **25**. These data show that the latter process is disfavored over the former one. Thus, the Me model which is in good agreement with the experimental result at this point (Scheme 1, conversion of **1b** into **2b**) will be retained for the latter calculations concerned with the Diels−Alder reactions. This definitely demonstrates that the ester groups play an active part in the chemical reactions; replacing them with methyl groups leads to good modeling approximations.
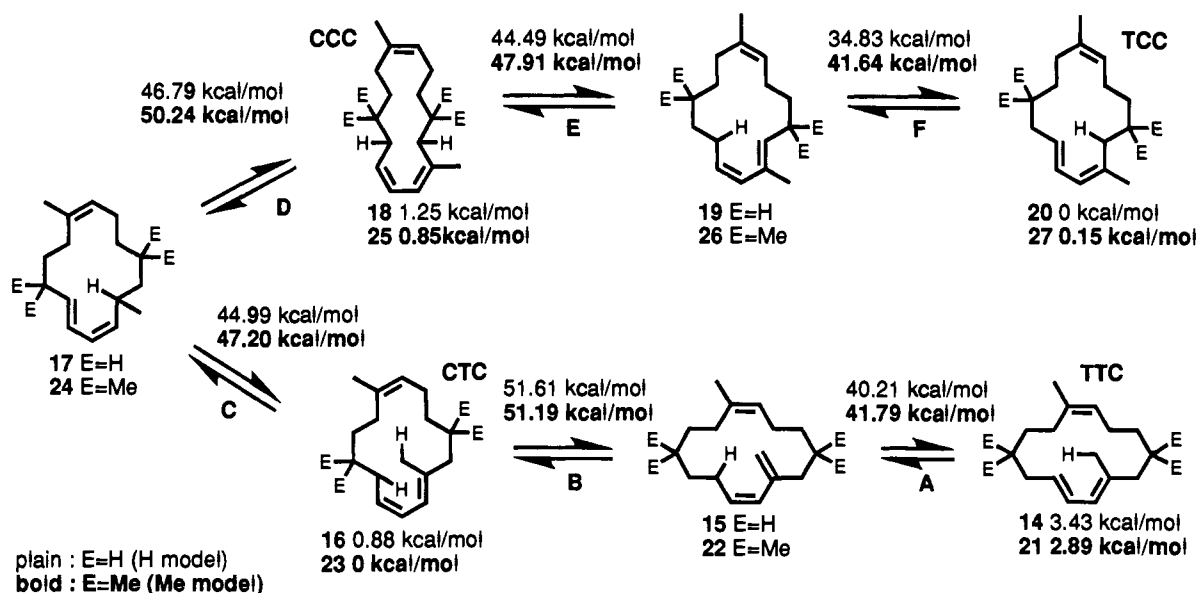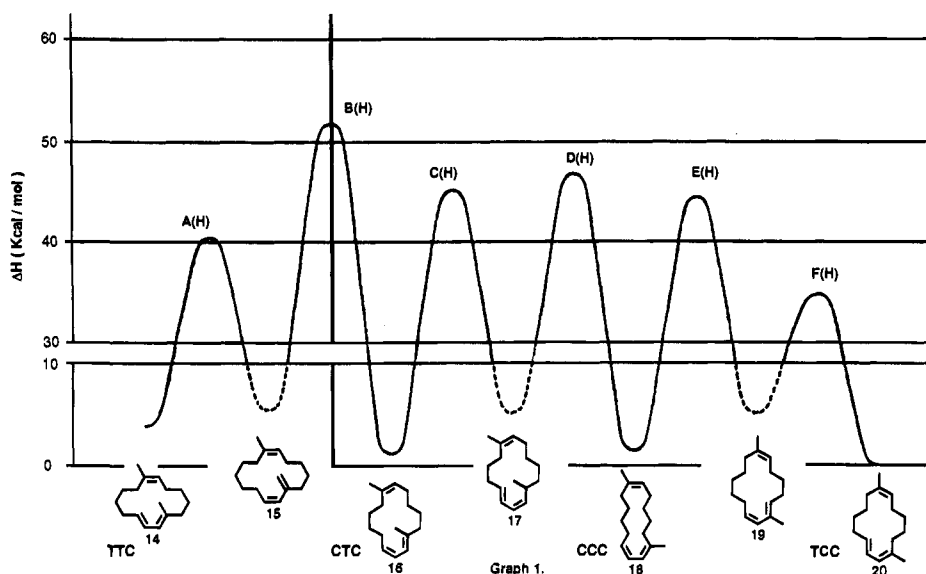
Scheme 4

E=CO$_2$Me. R groups are tethered by macrocyclic rings.

Pericyclic Reactions

J. Am. Chem. Soc., Vol. 117, No. 1, 1995 521

Scheme 5

CCC 44.49 kcal/mol / 47.91 kcal/mol → E → 34.83 kcal/mol / 41.64 kcal/mol → F → TCC

46.79 kcal/mol / 50.24 kcal/mol ↕ D

18 1.25 kcal/mol / **25** 0.85 kcal/mol

19 E=H / **26** E=Me

20 0 kcal/mol / **27** 0.15 kcal/mol

17 E=H / **24** E=Me

44.99 kcal/mol / 47.20 kcal/mol ↕ C

CTC 51.61 kcal/mol / 51.19 kcal/mol → B → 40.21 kcal/mol / 41.79 kcal/mol → A → TTC

16 0.88 kcal/mol / **23** 0 kcal/mol

15 E=H / **22** E=Me

14 3.43 kcal/mol / **21** 2.89 kcal/mol

plain : E=H (H model)
bold : E=Me (Me model)

Chart 1. Energy profile of the macrocycles interconversions via [1,5]sigmatropic hydrogen shifts (see Scheme 5, H model).

Graph 1.

The Diels—Alder Reactions

All the macrocycles (**21**—**27**) (Scheme 6) can in principle undergo Diels—Alder cycloadditions apart from **22** for which

(5) Dewar, M. J. S.; Zoebisch, E. G.; Healy, E. F.; Stewart, J. J. P. *J. Am. Chem. Soc.* **1985**, *107*, 3902.

(6) Stewart, J. J. P. *J. Comput. Chem.* **1989**, *10*, 209 and 221.
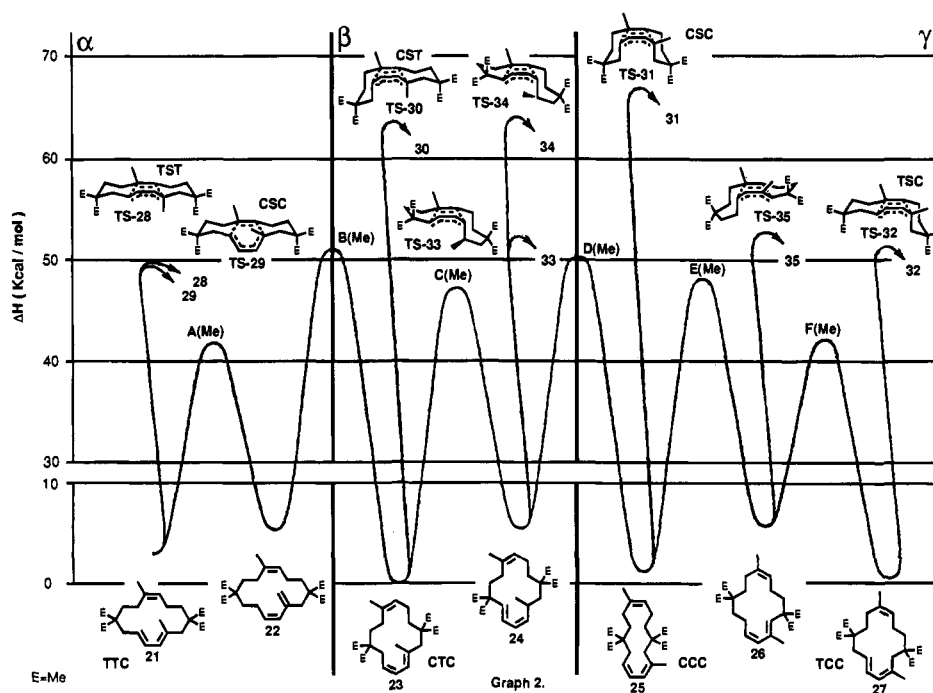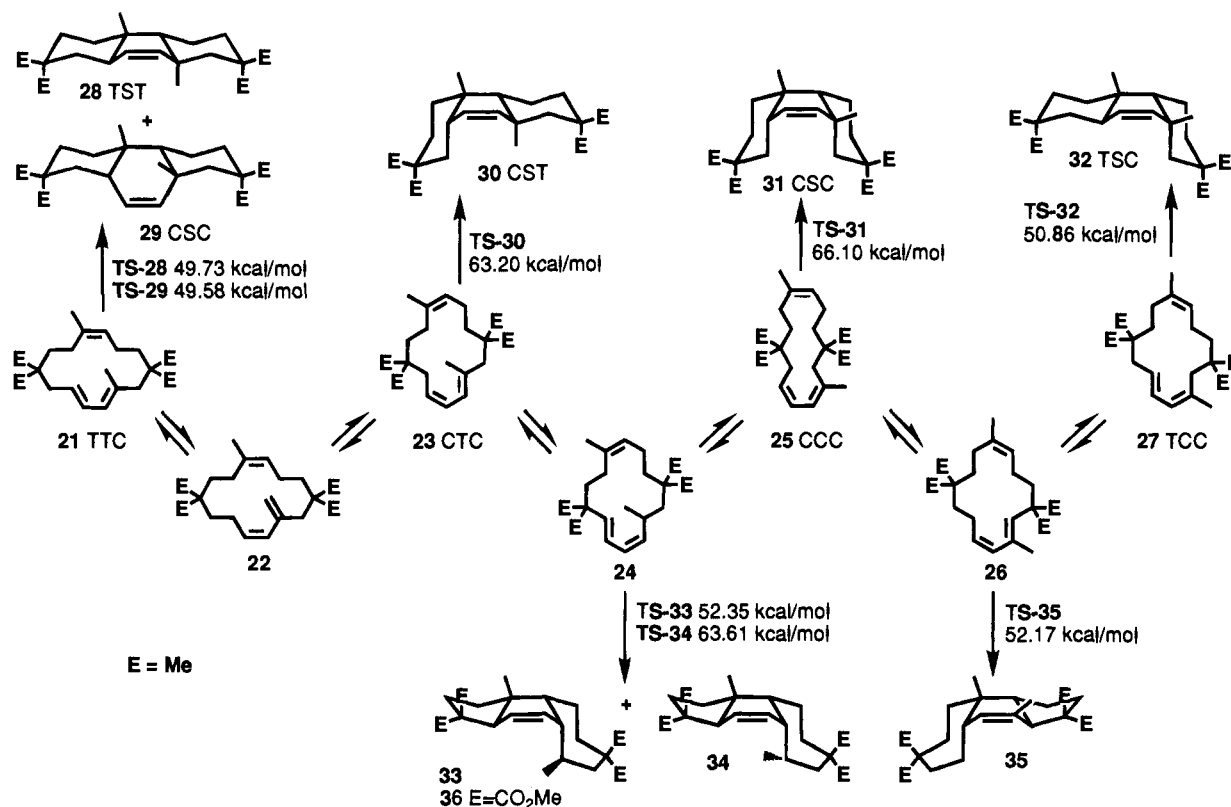
(7) Stewart, J. J. P. *QCPE No. 455*.

(8) Computational procedure: All the calculations were done at the RHF level. The first input files for MOPAC 6.00 were created by means of SYBYL 6.01 (Tripos Associates, Inc.: 16995 Hanley Rd, Suite 303, St. Louis, MO 63144-2913) for IBM RS/6000 computers. The gradients of the norm of these draft structures were then fully optimized using EF or TS subroutines. Finally, all the transition structures were characterized by only one negative force constant.

(9) Houk, K. N.; Li, Y.; Evanseck, J. D. *Angew. Chem., Int. Ed. Engl.* **1992**, *31*, 682.

(10) The X-ray structure of the macrocycle **3b** was available: its backbone coordinates were used as starting geometries to obtain the AM1 optimized structures of the macrocycles **16**, **23** (CTC), **20**, and **27** (TCC). Ring searches technics within SYBYL 6.01 were used to generate several low-energy TTC and CCC macrocyclic structures, which were then submitted to MOPAC 6.00 to get the macrocyclic geometries **14**, **21** (TTC), **18**, and **25** (CCC). No searches were carried out on the macrocycles **15**, **17**, **19**, **22**, **24**, and **26**. Michel, A. G.; Michel-Dewez, N.; Roughton, A. L.; Springer, J. P.; Hoogsteer, K. *Acta Crystallogr.* **1989**, *C45*, 932.

no viable Diels—Alder transition geometry exists. The transition structures (**TS-28**—**TS-35**) have been all calculated (E = Me) and their energies reported in Chart 2. It appears clearly that the three transition states **TS-30**, **TS-31**, and **TS-34** are completely ruled out, being too high in energy by at least 10 kcal/mol as compare with the five remaining Diels—Alder transition states **TS-28**, **TS-29**, **TS-32**, **TS-33**, and **TS-35**. These preliminary results contradict the available experimental data[3] since the compound **6b** had been tentatively assigned as the CST tricycle arising from a Diels—Alder transition structure similar to **TS-30**. Moreover, much to our surprise the 5—6—7- and 7—6—5-membered tricyclic transition structures **TS-33** and **TS-35** are calculated to be of similar energy to the 6—6—6-membered tricyclic transition structures **TS-28**, **TS-29**, and **TS-32** (≈2—3 kcal/mol gaps).

As a result of these calculations, the identity of the product **6b** was reexamined. The compound was tediously purified and the spectra confirmed that **6b** could not be the CST tricyclic Diels—Alder adduct related to the tricycle **30**. Rather, one of the methyl groups appearing as a doublet in the NMR spectrum (benzene) showed that **6b** is in fact the 5—6—7 tricycle **36**

Chart 2. Energy profile of the macrocycles interconversions (see Scheme 5, Me model) and competing Diels—Alder reactions[1] (see Scheme 6).

Graph 2.

Scheme 6

TS-28 49.73 kcal/mol
TS-29 49.58 kcal/mol

TS-30
63.20 kcal/mol

TS-31
66.10 kcal/mol

TS-32
50.86 kcal/mol

TS-33 52.35 kcal/mol
TS-34 63.61 kcal/mol

TS-35
52.17 kcal/mol

E = Me

36 E=CO₂Me

corresponding to the tricycle **33** (Scheme 6). Its identity was clearly established by X-ray structure analysis (Figure 3). It is therefore very interesting to note that the calculations reproduce remarkably well at least qualitatively the experimental results: out of the five calculated possible Diels—Alder adducts **28**, **29**, **32**, **33**, and **35**), four of them have been detected experimentally (E = CO₂Me instead of Me).

Considering the fact that the [1,5]hydrogen shift reactions are reversible, they act as configurational barriers between the

seven macrocycles **21–27**. It is known that when reversible conformational (configurational in the present case) barriers are well below irreversible reactions barriers, the Curtin—Hammett principle applies. The opposite situation leads to a case known as the case of conformational equilibrium control, which solution is also straightforward. The problem is, however, much more difficult to handle when the reversible conformational and the irreversible reaction barriers are in the same energy region.[11]

(11) Zefirov, N. S. *Tetrahedron* **1977**, *33*, 2719.

21 (2.89)

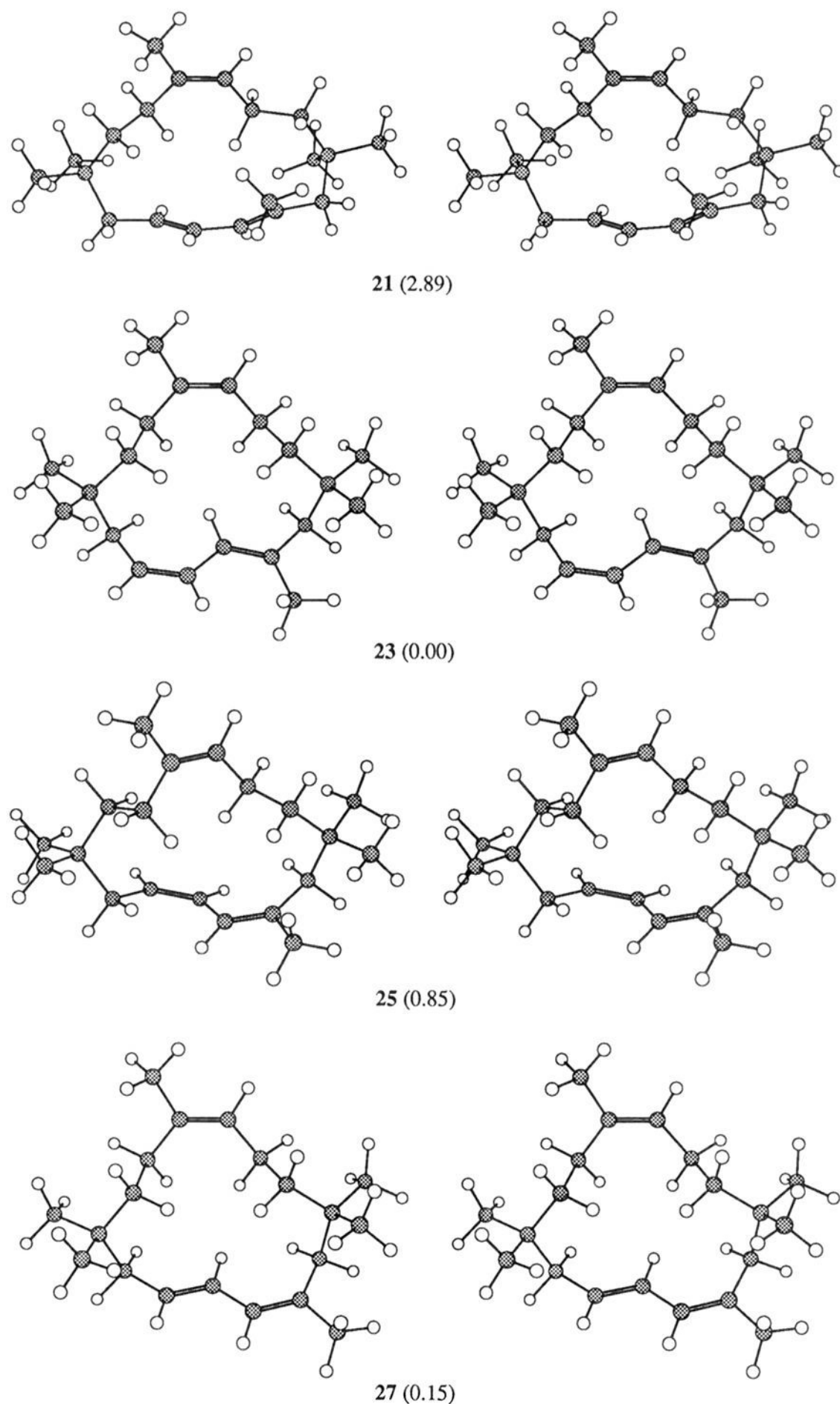**23** (0.00)

25 (0.85)

27 (0.15)

Figure 1. Stereoviews of the macriocycles **21** (TTC), **23** (CTC), **25** (CCC), and **27** (TCC). Energies in kcal/mol are indicated.

Such is particularly the case for the two highest [1,5]hydrogen shifts configurational barriers B(Me) and D(Me) (Chart 2) as suggested by the AM1 calculations. These two highest configurational barriers define three zones, α, β, and γ, inside which all the chemical processes obey the Curtin—Hammett principle. These considerations readily rationalize the experimental results. From the zone α, only two Diels—Alder transition states **TS-28** and **TS-29** may exist. As a result, treating the TTC macrocycle **21** under Diels—Alder conditions leads mainly (92%) to the two corresponding adducts. Also, since the [1,5]-hydrogen shift transition structure B(Me) is energetically close to these Diels—Alder transition structures, Diels—Alder adducts issued from the zones β (2%) and γ (6%) are also observed. Applying the same analysis to the zone B shows that the CTC macrocycle **23** should give mainly the 5—6—7-membered tricyclic adduct **33**; the two other transition structures **TS-30**

and **TS-34** are too high in energy and do not lead to products (Figure 4). Experimentally, the 5—6—7-membered tricycle **36** (Scheme 6) was the major product (60% of the mixture) formed beside Diels—Alder products coming from the zone α (20%) and γ (20%). This last result confirms that the configurational barriers B(Me) and D(Me) must be close to each other in energy. Also the Diels—Alder reaction leading to **33** accounting for only 60% in this case shows that it requires significantly more energy that the zone α Diels—Alder cases **28** and **29**. The calculations give a gap of about 2.5 kcal/mol favoring **TS-28** and **TS-29** over **TS-33**, again in good qualitative agreement with the experiments. Finally, from the zone γ, three adducts may in principle be formed from the TCC macrocycle **27** (Figure 5). The CSC transition structure **TS-31** is extremely disfavored and no CSC adduct can be formed through it. The remaining two transition structures **TS-32** and **TS-35** are separated by a 1.31
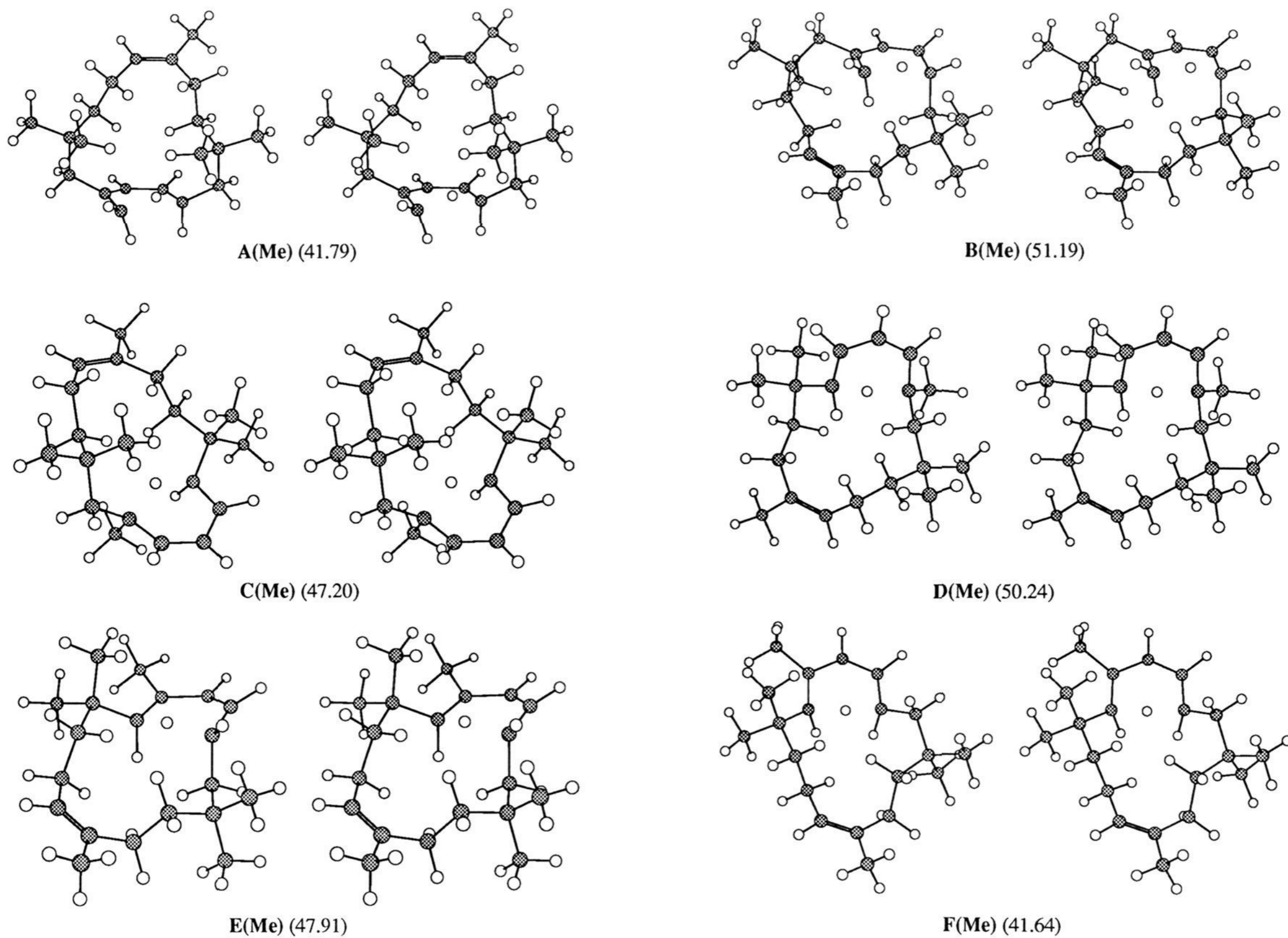
A(Me) (41.79)

B(Me) (51.19)

C(Me) (47.20)

D(Me) (50.24)

E(Me) (47.91)

F(Me) (41.64)

Figure 2. Stereoviews of the [1,5]sigmatropic hydrogen shift transition structures A(Me) to F(Me). Energies in kcal/mol are indicated.
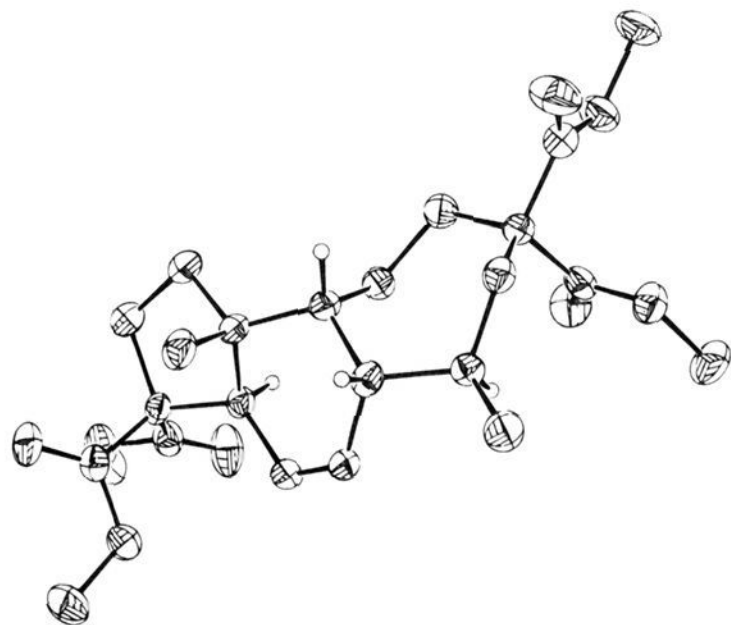
Figure 3. ORTEP drawing of **36**.

kcal/mol energy gap in favor of the TSC transition structure **32**. Experimentally, the TSC adduct **7b** (corresponding to the structure **32**) only was obtained, demonstrating that the calculations are again qualitatively right.
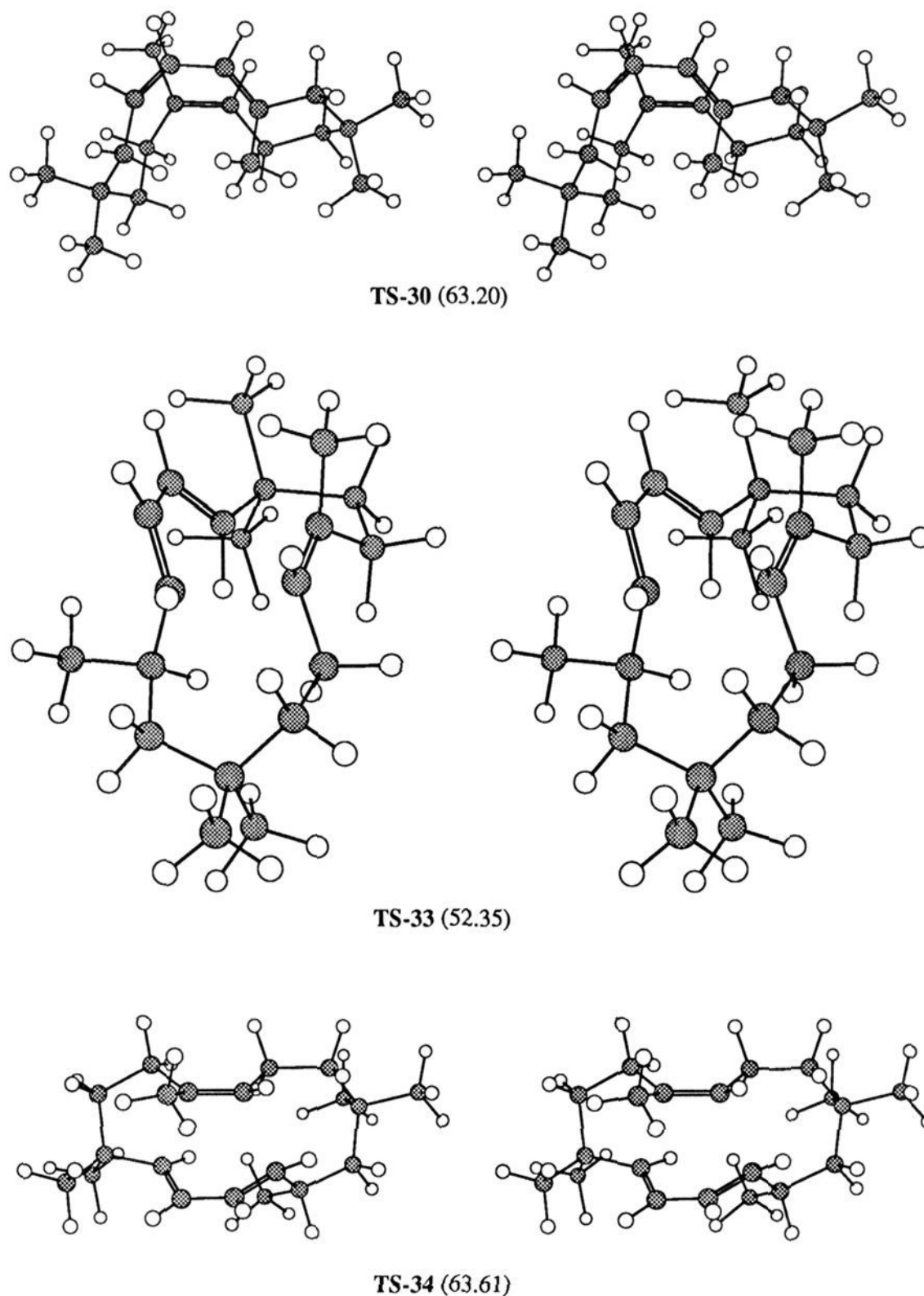
The TST/CSC Diels—Alder Adducts Ratios

The opposite TST/CSC Diels—Alder selectivity as a function of the EE diene substitution (TTC macrocycles **1a** and **1b**) is noteworthy. Thus, the unsubstituted diene **1a** (Scheme 1) leads to complete TST selectivity, whereas, its methyl-substituted equivalent **1b** yields the CSC tricycle **5b** as the major product. Since the TST/CSC ratios are identical starting either from the TTC macrocycle **1b** or the CTC macrocycle **2b**, it is then confirmed that the CSC tricycle is always formed via a transition state like **TS-29** rather than **TS-31** (Scheme 6).

All the transition structures responsible for the products formations were calculated by means of both the RHF semiempirical hamiltonians AM1 and PM3 (Schemes 7 and 8, Figures 6 and 7, all the energies quoted in these schemes and figures are relative energies, the lowest energy transition structures being always set to 0 kcal/mol), the ester groups being replaced by hydrogen atoms (E = H, AM1 and PM3) and methyl groups (E = Me, AM1 and PM3). In all cases the AM1 and PM3 values are very similar.[12] Thus, with the unsubstituted diene **1a** (Scheme 7) the TST preference is already forecast when the ester groups are replaced by hydrogen atoms (E = H, AM1, TST/CSC = $(91.2 + 0.4)/(8.2 + 0.2) \approx 92/8$). Not surprisingly
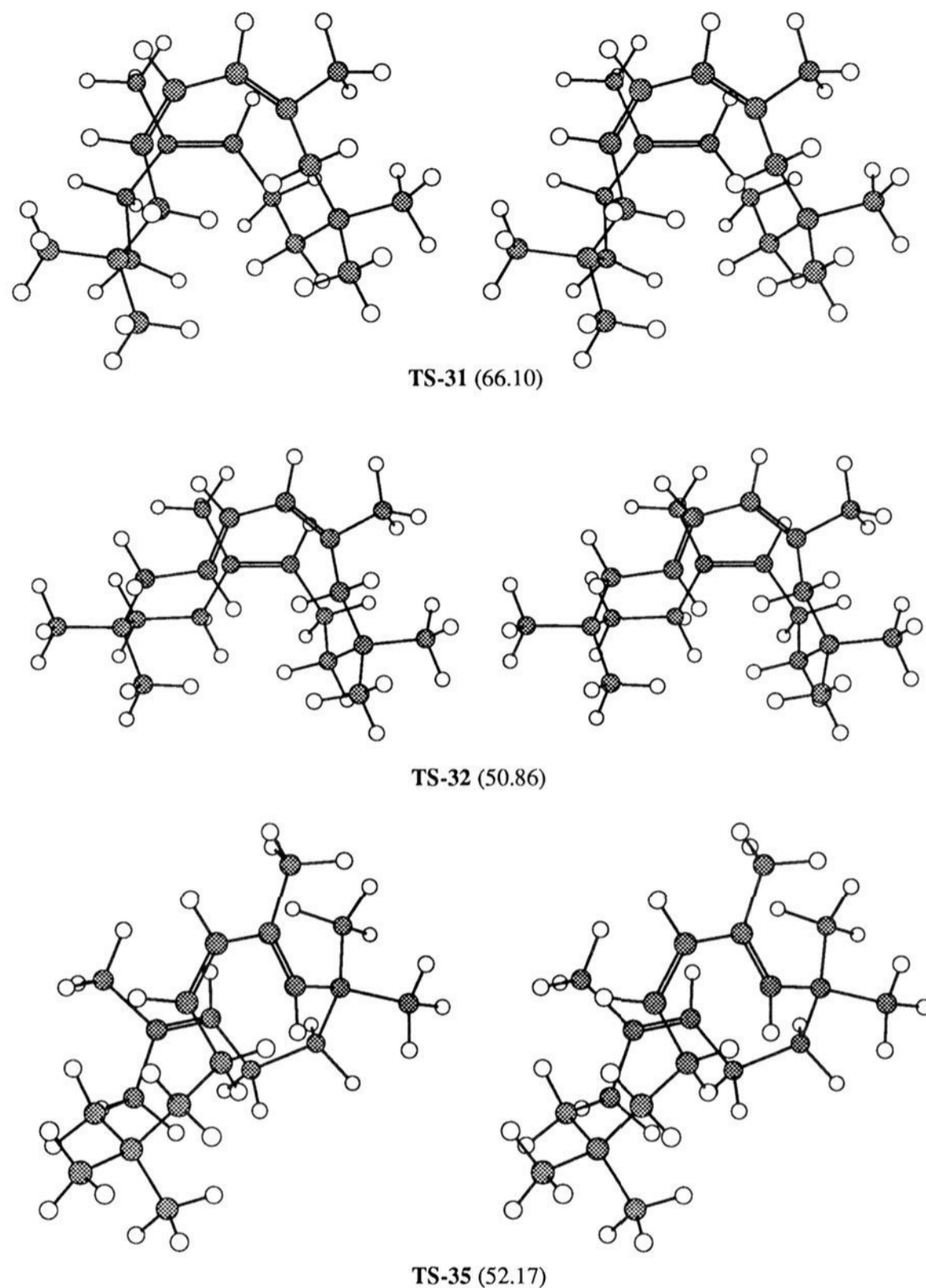

TS-30 (63.20)

TS-33 (52.35)

TS-34 (63.61)

Figure 4. Zone β Diels—Alder transition structures **TS-30**, **TS-33**, and **TS-34** (stereoviews). Energies in kcal/mol are indicated.

TS-31 (66.10)

TS-32 (50.86)

TS-35 (52.17)

Figure 5. Zone γ Diels−Alder transition structures **TS-31**, **TS-32**, and **TS-35** (stereoviews). Energies in kcal/mol are indicated.
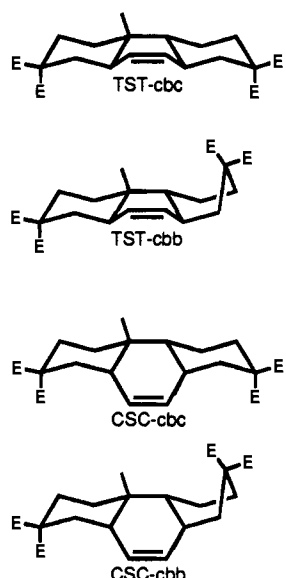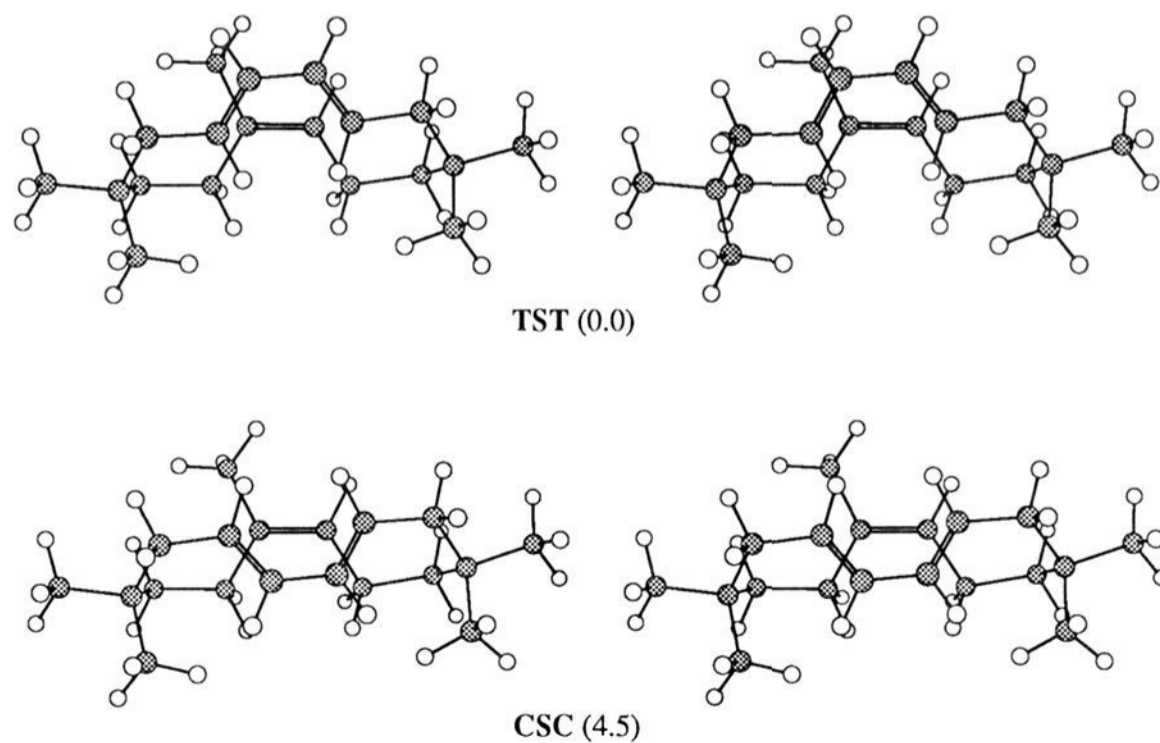

TST (0.0)

CSC (4.5)

Figure 6. Chair−boat−chair (cbc) AM1 transition structures (Scheme 7, E = Me) related to the Diels−Alder reaction of the macrocycle **1a** (stereoviews). Energies in kcal/mol are indicated.
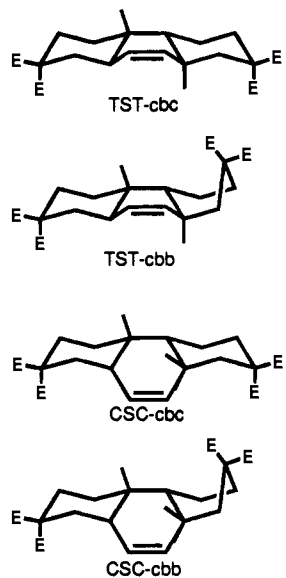
Pericyclic Reactions

J. Am. Chem. Soc., Vol. 117, No. 1, 1995 527

Scheme 7

80°C

	E=H				E=Me				E=CO₂Me
	AM1		PM3		AM1		PM3		Experiment
	ΔHF (kcal/mol)	ratio	ΔHF (kcal/mol)	ratio	ΔHF (kcal/mol)	ratio	ΔHF (kcal/mol)	ratio	ratio
TST-cbc	0	91.2%	0	91.1%	0	99.7%	0	98.9%	**TST**
TST-cbb	3.9	0.4%	3.6	0.6%	5.1	0.1%	4.1	0.3%	100%
CSC-cbc	1.7	8.2%	1.7	8.2%	4.5	0.2%	3.4	0.8%	**CSC**
CSC-cbb	4.3	0.2%	4.6	0.1%	7.9	/	7.0	/	/

Scheme 8

310°C

	E=H				E=Me				E=CO₂Me
	AM1		PM3		AM1		PM3		Experiment
	ΔHF (kcal/mol)	ratio	ΔHF (kcal/mol)	ratio	ΔHF (kcal/mol)	ratio	ΔHF (kcal/mol)	ratio	ratio
TST-cbc	1.2	22%	0.7	32%	0.1	41%	0.7	31%	**TST**
TST-cbb	4.5	1%	4.4	1%	2.8	4%	3.4	3%	15%
CSC-cbc	0	60%	0	58%	0	45%	0	56%	**CSC**
CSC-cbb	1.5	17%	2.2	9%	1.7	10%	2.0	10%	85%

TS-28 (cbc) (0.1)

TS-28 (cbb) (2.8)

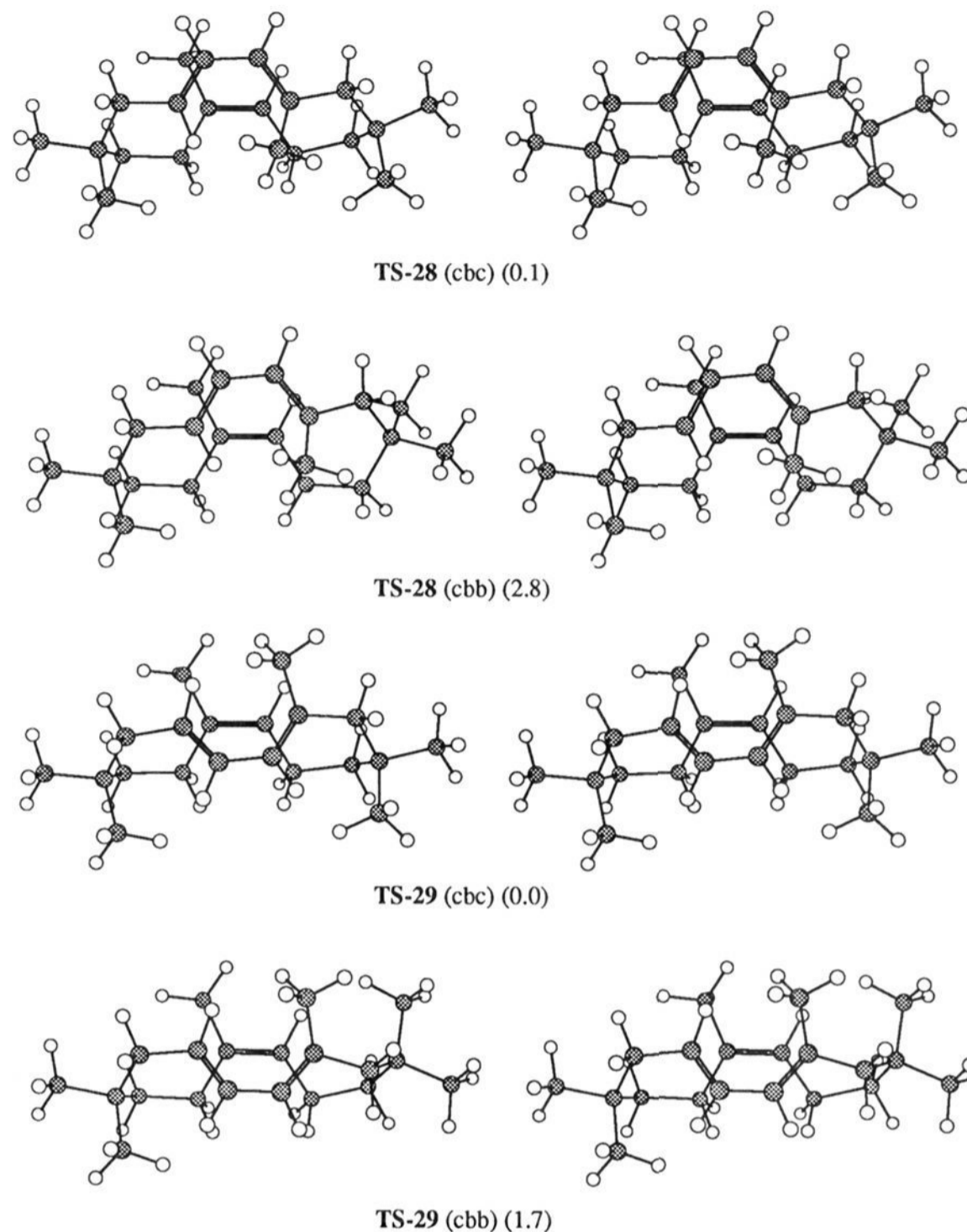**TS-29** (cbc) (0.0)

TS-29 (cbb) (1.7)

Figure 7. Zone α Diels−Alder AM1 transition structures (Scheme 8, E = Me) **TS-28** (cbc), **TS-28** (cbb), **TS-29** (cbc), and **TS-29** (cbb). Relative energies in kcal/mol are indicated.

the selectivity is enhanced (E = Me, AM1, TST/CSC = (99.7 + 0.1)/0.2 ≈ 100/0) when the methyl groups are added at the ester positions, because 1,3-diaxial interactions arise between these bulky groups and the diene in the CSC transition structures. It is worth noting that only chair−boat−chair transition structures (TST-cbc and CSC-cbc) have physical significance, compared to the chair−boat−boat competing geometries (TST-cbb and CSC-cbb).

In the case of the methyl substituted diene macrocycle **1b** (Scheme 8), the CSC preference experimentally observed (CSC: TST, 85:15) is already predicted when the esters are replaced by hydrogen atoms (E = H, AM1, TST/CSC = (22 + 1)/(60 + 17) = 23/77; PM3, TST/CSC = (32 + 1)/(58+9) = 33/67), and overall the modifications are marginal when the methyl groups are introduced (E = Me, AM1, TST/CSC = (41 + 4)/(45 + 10) = 45/55; PM3, TST/CSC = (31 + 3)/(56 + 10) = 34/66). Interestingly, the *cis-syn-cis* chair−boat−boat transition structures (CSC-cbc) account for as much as 17% (E = H, AM1) of the products. This phenomenon has already been observed for other systems where the tether boat ring was next to a *cis* forming ring function.[12,13]

---

(12) Dory, Y. L.; Ouellet, C.; Berthiaume, S.; Favre, A.; Deslongchamps, P. *Bull. Soc. Chim. Fr.* **1994**, *131*, 121.

(13) Coe, J. W.; Roush, W. R. *J. Org. Chem.* **1989**, *54*, 915.

Conclusion

We have clearly demonstrated that complex selectivity problems involving different competing mechanisms (*e.g.* [1,5]-sigmatropic hydrogen shifts and Diels−Alder cycloadditions) can be successfully handled by means of semiempirical quantum mechanics calculations. Thus, the calculations have (Chart 2, Scheme 1) allowed us to identify two macrocycles interconversion barriers ([1,5]sigmatropic hydrogen shift transition structures B(Me) and D(Me) whose activation enthalpies are near all the feasible Diels−Alder activation enthalpies transition structures (**TS-28**, **TS-29**, **TS-32**, **TS-33**, and **TS-35**). As a result, the whole system is divided into three zones, α, β, and γ, where the Curtin−Hammett principle is valid. From the zone α, both macrocycles **21** and **22** should in principle yield mainly the two tricyclic Diels−Alder adducts **28** and **29**, **29** being the major adduct. The two zone β macrocycles **23** and **24** give chiefly one adduct: the 5−6−7-membered tricycle **33**, whereas the three zone γ macrocycles **25**−**27** produce **32** as the major Diels−Alder adduct. All these calculations conclusions (Chart 2, E = Me) are shown to be experimentally confirmed (Scheme 1, E = CO₂Me). One of the previously missassigned adduct **6b** (corresponding to **TS-30**) was found to be the 5−6−7 tricyclic adduct corresponding to **TS-33**. Therefore, the method is extremely powerful in the case of transannular Diels−Alder

reactions, since it can help correcting ambiguous structures assignments and predicting the outcomes of all our transannular Diels—Alder-based strategies.

Experimental Section

Purification of the Tricycle 36. The crude product (7.0 mg) issued from the treatment of the CTC macrocyclic triene **2b** at 325 °C[2] was purified by preparative chromatography on a plate of silica gel (0.5 mm, Kieselgel 60 F$_{254}$). The plate was eluted twice with a mixture (2:98) of acetone (distilled) and toluene (distilled over sodium) to yield the tricycle Diels—Alder adduct **36** (2.1 mg). The product was crystallized once from ether (distilled) and hexane (distilled) then from methanol (distilled over methyl magnesium iodide): mp (Büchi-M-50) (uncorrected) 153—155 °C; ^{1}H NMR (δ, C$_6$D$_6$, 250 MHz) (Bruker WM-250) 0.86 (3H, s, C*Me*), 1.00 (3H, d, J = 6.6 Hz, CH*Me*), 1.14 (1H, ddd, J = 1.8, 8.9, 10.7 Hz, C*H*H), 1.34 (1H, m, CH*Me*), 1.35—1.6 (5H, m, C*H*H and CHC*H*CMe), 1.97 (1H, m, C*H*CHMe), 2.1—2.35 (3H, m, C*H*H), 2.82, (1H, m, C*H*H), 2.96 (1H, m, MeC-C*H*CH=CH), 3.12 (1H, td, J = 8.9 Hz, 14.4 Hz, C*H*H), 3.28 (3H, s, CO$_2$*Me*), 3.29 (3H, s, CO$_2$*Me*), 3.34 (3H, s, CO$_2$*Me*), 3.37 (3H, s, CO$_2$*Me*), 5.48 (1H, br d, J = 10.4 Hz, C*H*=CH), 6.31 (1H, td, J = 2.2, 10.4 Hz, CH=C*H*); HRMS (EI) (Micromass ZAB-2F) calculated for C$_{24}$H$_{34}$O$_8$ 450.2257, found 450.2254.

Supplementary Material Available: Full X-ray data of compound **36** and all MOPAC archive files corresponding to the structures shown in the figures (22 files) (61 pages). This material is contained in many libraries on microfiche, immediately follows this article in the microfilm version of the journal, and can be ordered from the ACS; see any current masthead page for ordering information.

JA9422930